Mimicking glide-symmetry dispersion with coupled slot metasurfaces

Miguel Camacho,[1, a)] Rhiannon C. Mitchell-Thomas,[1] Alastair P. Hibbins,[1] J. Roy Sambles,[1] and Oscar Quevedo-Teruel[2]

[1)] *Electromagnetic and Acoustic Materials Group, Department of Physics and Astronomy, University of Exeter, Stocker Road, Exeter EX4 4QL, United Kingdom*

[2)] *Department of Electromagnetic Engineering, KTH Royal Institute of Technology, SE, 100 44, Stockholm, Sweden*

In this Letter we demonstrate that the dispersion properties associated with glide symmetry can be achieved in systems that only possess reflection symmetry by balancing the influence of two sub-lattices. We apply this approach to a pair of coupled slots cut into an infinite perfectly conducting plane. Each slot is notched on either edge, with the complete two-slot system having only mirror symmetry. By modifying the relative size of the notches on either side of the slots, we show that a linear dispersion relation with a degeneracy with non-zero group velocity at the Brillouin zone boundary can be achieved. These properties, until now, only found in systems with glide symmetry are numerically and experimentally validated. We also show that these results can be used for the design of ultra-wideband one-dimensional leaky wave antennas in coplanar waveguide technology.

Periodic structures that possess a higher symmetry, such as glide (consisting of a reflection and a translation) or twist (consisting of a rotation and a translation) symmetries, are those that are invariant with respect to a more complex operation than either a reflection or a translation.[1] It was shown by Crepeau *et al.* and later by Hessel *et al.*, that systems showing such symmetries present a dispersion relation that appears to correspond to an effective unit cell which is half of that defined by the geometry.[2]

It was not until recently that this property started being exploited for metasurfaces, due to the quasi-linear dispersion relation obtained for systems with higher symmetries. With this property, metasurfaces showing low dispersion can be achieved,[3–5] meaning that surface waves supported by these patterned surfaces behave as if they were propagating in a medium with a constant refractive index over a broad range of frequencies.

Removing the strong frequency dependence of the behaviour of metasurfaces provides a route towards broadband surface wave lensing[6] or improved leaky wave control for antennas.[7,8] In addition, due to the high effective refractive index found in glide symmetric structures, large band-gaps can be achieved between higher and lower order modes, with important applications for integrated waveguides.[9,10] These high effective indices are accompanied by degeneracies at the Brillouin zone boundary which have the potential to create reconfigurable band-gap materials. In most studies of glide symmetric metasurfaces, the authors made use of two-layer systems, with each of the layers patterned so that one of the surfaces is obtained through a glide operation (consisting of a reflection with respect to a plane between the two layers and a translation of half the unit cell).[3,4,9] Only recent work has been reported of the application of glide symmetry to ultra-thin single-layered metasurfaces.[11]

[a)] Electronic mail: mc586@exeter.ac.uk

The possibility of achieving zero bandgaps with non-zero group velocity at the high symmetry points of the dispersion relation in metamaterials has attracted much attention. In leaky wave antennas, broadside radiation can be achieved for instance by closing the bangap for zero in-plane momentum.[12,13] In the context of topological photonics, the study of such bandgap closures has important implications in the creation of interface states with large field enhancements.[14,15]

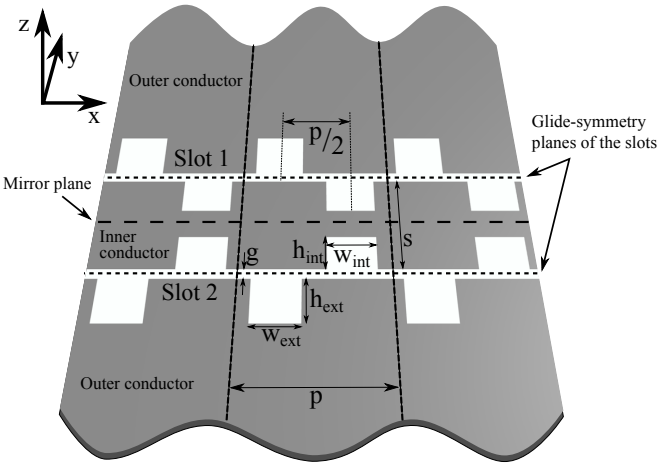

FIG. 1. Perspective view of the negligible thickness conducting plane perforated with a pair of coupled slots with glide-symmetric notches. The glide-symmetry plane for each of the slots has been represented by a short-dashed line while the long-dashed line represents global mirror plane of the system.

In the work presented here, we show that the concept of glide symmetry can be used to reduce the frequency dependence of the mode index without the presence of any higher symmetry. This concept is applied to a pair of infinitely long coupled slots in an ground plane which is the simplest two-dimensional system that supports, at any frequency, the propagation of bound modes.[16,17] The ground plane is here assumed to be perfectly conduct-

ing and of negligible thickness, common and accurate assumption at microwave frequencies. Due to the symmetry of the waveguide, this two-slot system supports two families of modes, each of which exhibits either even or odd parity for the transverse in-plane electric field component with respect to the symmetry plane of the configuration. In general, only the odd mode (commonly known as the coplanar waveguide mode) is used for propagation, which can be readily excited by connecting the two outer conductors to ground and applying an oscillating signal to the central strip. In contrast, the even mode, in the presence of a thick dielectric superstrate, is used for leaky wave applications.[18] Both modes lie on the lightline (representing the dispersion relation of a grazing plane wave) due to the translational symmetry along the x-direction.

By the addition of periodic notches to both infinitely long slots, the momentum of the bound mode can be increased obtaining a pseudo-plasmonic dispersion. These bound surface modes conventionally have band gaps and zero group velocity at the Brillouin zone boundary. However, as shown for multi-layered structures, when applying a glide operation to metasurfaces that support pseudo-plasmonic dispersion, one can linearize the dispersion and introduce a degeneracy between the two lowest order modes of the system at the Brillouin zone boundary, therefore considerably increasing the bandwidth of operation.[3]

In Fig. 1, the doubly-notched slot pair is shown. Each of the two slots has been patterned by introducing rectangular notches in both the inner and outer conductors. As can be seen, for each of the two infinite slots, for the case of inner and outer notches of the same size, each of the two slots presents a glide-symmetric geometry. Then, the second patterned slot can be obtained through a reflection operation of the first. Although each of the individual patterned slots presents glide symmetry, the patterned surface does not exhibit any higher symmetry due to the central mirror plane. This allows the parity of the transverse in-plane electric field component to be conserved, and therefore the radiative behavior of the even and odd modes remains unchanged.[18] The separation between even and odd modes introduced by the mirror symmetry significantly reduces the complexity of the excitation mechanism, important for practical applications.

In the following we show that even in the absence of geometrical glide symmetry, one can design a system to show the exact same characteristics namely a degeneracy at the Brillouin zone boundary with non-zero group velocity that leads to a linear dispersion relation. To do this, we modify the relative sizes of the inner and outer notches to balance their dispersion properties. In general, a band repulsion would occur, forbidding the existence of a crossing point. In our case, however, the bandgap closes thanks to the inversion symmetry plane of the system parallel to the x and z axes at the centre of the notches, which allows for the two bands to merge as theoretically demonstrated for the case of one dimensional periodically stacked photonic crystals.[14] In the absence of such inversion-symmetry plane, further modelling (using rectangular triangules as notches) has shown that the bandgap cannot be closed. However, the linearity of the dispersion relation for frequencies below the gap can be greatly improved by minimizing the bandgap.

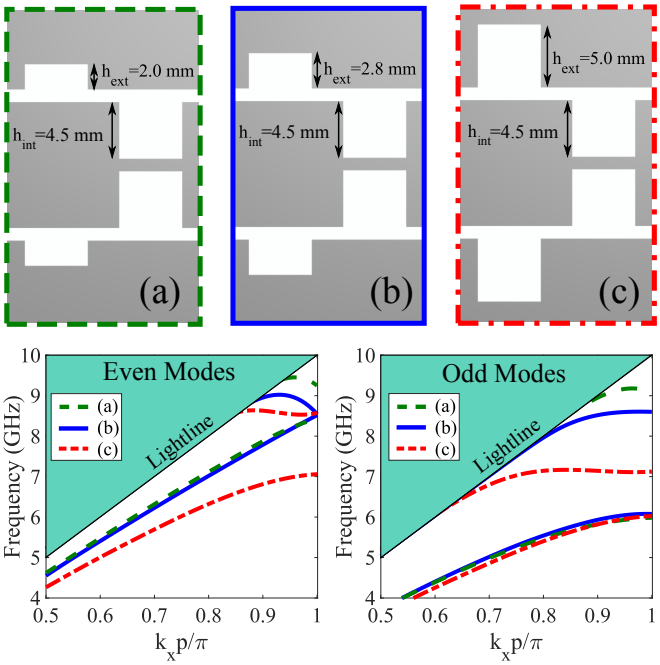

FIG. 2. Prediction of the dispersion of both even and odd modes for different h_{ext}, evolving to the effective glide symmetry characteristics for the even modes. The top three boxed figures represent the unit cell geometry for each of the three dispersion diagrams presented. The bottom left (right) figure shows the dispersion diagram obtained for the even (odd) bound modes supported by the coupled slot system. The values of the other parameters are $h_{\text{int}} = 4.5\,\text{mm}$, $w_{\text{ext}} = w_{\text{int}} = 5\,\text{mm}$, $s = 10\,\text{mm}$, $g = 1\,\text{mm}$ and $p = 15\,\text{mm}$.

Fig. 2 shows the modelled dispersion for different heights of the outer notch, with the height of the inner notch, h_{int}, kept constant at 4.5 mm ($h_{\text{ext}}/h_{\text{int}} \approx 0.62$). It can be seen that the band-gap present at the first Brillouin zone boundary for both even and odd modes can be tuned by the size of the outer notch. Moreover, for the even mode, the band-gap can be closed for $h_{\text{ext}} = 2.8\,\text{mm}$ with the two degenerate modes presenting non-zero group velocity at the Brillouin zone boundary. The linear dispersion (for the even modes) is apparent: compare the solid blue line (associated to the effective glide symmetry) to the red dash-dotted line (non symmetric case). This case corresponds to a nearly constant mode index of 1.2 for frequencies up to 9 GHz. It can also be seen from the green dashed curve that even when the effects introduced by the two sub-lattices are not exactly balanced, an important improvement in the linearity of the dispersion may be obtained. In contrast, for the odd

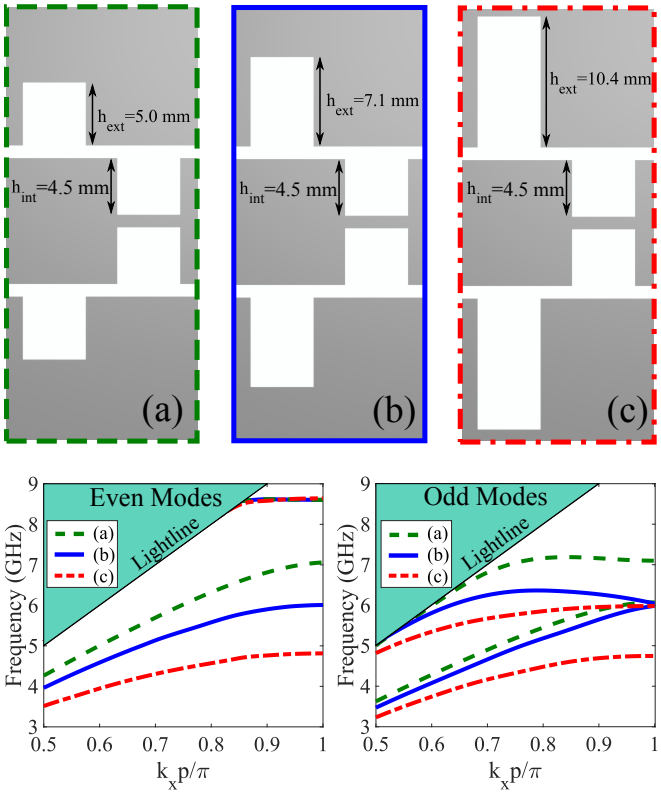

FIG. 3. Dispersion diagrams modelled for both even and odd modes for different h_{ext}, evolving to the effective glide symmetry characteristics for the odd modes. The top three boxed figures represent the unit cell geometry for each of the three dispersion diagrams presented. The bottom left (right) figure shows the dispersion diagram obtained for the even (odd) bound modes supported by the coupled slot system. The values of the other parameters are $h_{\text{int}} = 4.5\,\text{mm}$, $w_{\text{ext}} = w_{\text{int}} = 5\,\text{mm}$, $s = 10\,\text{mm}$, $g = 1\,\text{mm}$ and $p = 15\,\text{mm}$.

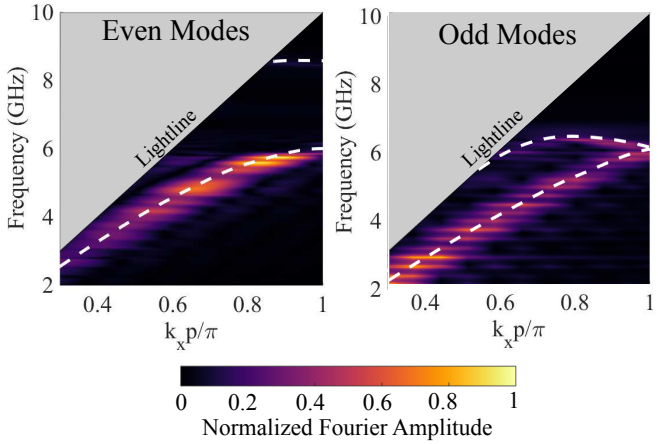

FIG. 4. Experimental and modelled dispersion diagrams for both even and odd modes of the coupled slot system. The colormap background represents the Fourier amplitude obtained from the fast Fourier transform of the measured field distribution and the superimposed white dashed lines represent the modelled dispersion relation. The values of the parameters are $h_{\text{ext}} = 7.1\,\text{mm}$, $h_{\text{int}} = 4.5\,\text{mm}$, $w_{\text{ext}} = w_{\text{int}} = 5\,\text{mm}$, $s = 10\,\text{mm}$, $g = 1\,\text{mm}$ and $p = 15\,\text{mm}$.

modes, the lowest order mode is not significantly affected, due to the bigger energy gap between the two lowest order modes, although some linearization of the dispersion with respect to the single notched system is found far from the Brillouin zone boundary. Following the same procedure, the band-gap at the Brillouin zone boundary may also be removed for the odd modes. Due to the lowest order odd mode crossing the Brillouin zone boundary at a lower frequency, the closure of the band-gap for the odd modes is achieved for larger values of h_{ext} than in the previous case. In Fig. 3, it can be seen that this occurs for $h_{\text{ext}} = 7.1\,\text{mm}$, for which a very linear dispersion is obtained due to the non-zero group velocity obtained at the Brillouin zone boundary (where the modes are degenerate). In the case of the odd mode, the ratio between sizes that mimics the glide-symmetric behaviour is $h_{\text{ext}}/h_{\text{int}} \approx 1.6$, which is close to the inverse of that obtained for the effective glide symmetry case for the even mode.

To validate the results obtained from commercial software,[19] experimental measurements have been undertaken for the case of a structure having zero band-gap in the odd mode (solid blue line in Fig. 3). The sample was manufactured using a print and etch technique applied to a 17 µm thick copper layer on a 23 µm thick plastic substrate with a relative dielectric permeability of 2.8. The even and odd modes of the system were excited in two different experiments, and in each the field distribution was measured by scanning the surface with a modified coaxial antenna in the near field. By using a Fast Fourier Transform algorithm to transform the spatial dependence of the measured fields into the reciprocal space, the experimental dispersion diagrams of Fig. 4 have been obtained for both even and odd modes.[20] Additionally, the simulated eigenmode solutions have been plotted for comparison purposes showing a good agreement. The effective mode index of 2.2 is nearly constant up to 6 GHz.

The experimental and simulated in-plane electric field distributions have been plotted in Figs 5 and 6 for the even and odd modes respectively. To obtain these, the in-plane field component was extracted from the measurement of a coaxial cable terminated with a pair of parallel wires, which captured the contribution from both the in-plane and out-of-plane components. This extraction was possible due to the different parity of the two electric field components with respect to the centre of the structure. Although not easily noticeable in the experimental dispersion diagram for the even mode, the existence of the second mode is proven by the measured field distribution at 8.5 GHz in Fig. 5. Note that the effective in-plane wavelength measured for the two modes matches that of the simulated structure.

Finally, we show that by taking advantage of the lin-

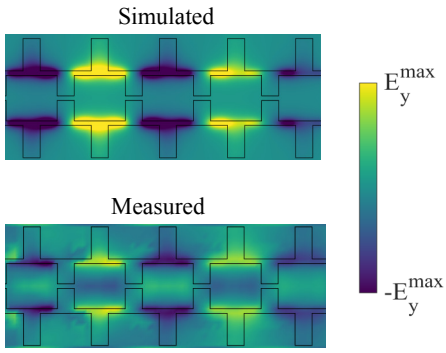

FIG. 5. Experimental and modelled y component of the electric field distribution along four and a half consecutive unit cells when exciting the even mode at 8.5 GHz. The values of the parameters are $h_{\text{ext}} = 4.5\,\text{mm}$, $h_{\text{int}} = 4.5\,\text{mm}$, $w_{\text{ext}} = w_{\text{int}} = 5\,\text{mm}$, $s = 10\,\text{mm}$, $g = 1\,\text{mm}$ and $p = 15\,\text{mm}$.

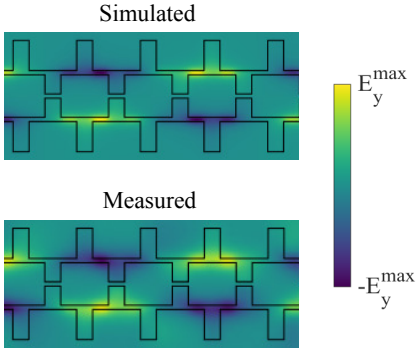

FIG. 6. Experimental and modelled y component of the electric field distribution along four and a half consecutive unit cells when exciting the odd mode at 4 GHz. The values of the parameters are $h_{\text{ext}} = 4.5\,\text{mm}$, $h_{\text{int}} = 4.5\,\text{mm}$, $w_{\text{ext}} = w_{\text{int}} = 5\,\text{mm}$, $s = 10\,\text{mm}$, $g = 1\,\text{mm}$ and $p = 15\,\text{mm}$.

earized dispersion achieved before, one can design a one-dimensional ultra-wideband leaky wave antenna. It is known that, in the presence of a dense material, the evanescent fields of the bound modes can be turned into propagative.[21] In general, the leakage will produce a beam centered at an elevation angle given by $\gamma = \arccos\left(k_1/k_o^d\right)$ where k_1 is the momentum of the bound mode (which by adding a thin air-gap can be approximated as that in the absence of dielectrics) and k_o^d is the wavenumber in the denser medium.[8] In Fig. 7, we compare the elevation angle found for the case of zero and non-zero bandgap at the Brillouin zone boundary for the even mode. We find that in the case of zero-bandgap, the linearization of the dispersion allows for a nearly-constant elevation angle in a very large frequency band from DC up to 8 GHz. In contrast, the dispersive mode index found in the unbalanced case produces much larger changes in the elevation angle leading to a frequency dependent radiation pattern which is not desirable for practical applications.

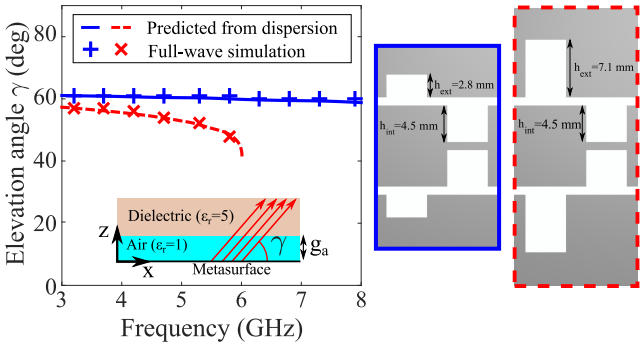

FIG. 7. Comparison of the frequency dependence of the elevation angle in the presence of a dielectric half-space of $\epsilon_r = 5$ for the cases of zero and non-zero bandgap in the even mode dispersion. The thick lines have been obtained from the dispersion relation in the absence of dielectrics and the crosses from full-wave simulations of the antenna. The values of the geometrical parameters are $h_{\text{ext}} = 4.5\,\text{mm}$, $h_{\text{int}} = 4.5\,\text{mm}$, $w_{\text{ext}} = w_{\text{int}} = 5\,\text{mm}$, $s = 10\,\text{mm}$, $g = 1\,\text{mm}$, $g_a = 30\,\text{mm}$ and $p = 15\,\text{mm}$.

In conclusion, we have shown that the family of structures that benefit from the use of higher symmetries can be extended to systems that present lower symmetries. Particularly in the case of a pair of coupled slots, the width of each infinitely long slot has been modulated in a glide symmetric fashion by introducing notches in both inner and outer conductors. However, due to the mirror symmetry imposed in the transmission line that allows the separation between even and odd modes, the two slot system does not possess glide symmetry. We have shown that by introducing an asymmetry between the sizes of the outer and inner notches, one can vastly improve the linearity of the dispersion relation of the surface modes supported by the coupled slots thanks to the introduction of a degeneracy with non-zero group velocity at the Brillouin zone boundary. This is in agreement with the previously reported behaviour of glide symmetric designs, obtaining an effective glide symmetry in a geometry that does not possess any higher symmetry. These results have been applied to the design of a ultra-wideband leaky-wave antenna that takes advantage of the widely used coplanar waveguide technology, largely reducing the complexity of the 'feed' necessary for previous multi-layered glide symmetric metasurfaces.

The authors wish to acknowledge financial support from the Engineering and Physical Sciences Research Council (EPSRC) of the United Kingdom, via the EPSRC Centre for Doctoral Training in Metamaterials (Grant No. EP/L015331/1). All data created during this research are openly available from the University of Exeter's institutional repository at https://ore.exeter.ac.uk/.

[1] P. Crepeau and P. McIsaac, Proceedings of the IEEE **52**, 33 (1964).

[2] A. Hessel, Ming Hui Chen, R. Li, and A. Oliner, Proceedings of the IEEE **61**, 183 (1973).
[3] O. Quevedo-Teruel, M. Ebrahimpouri, and M. Ng Mou Kehn, IEEE Antennas and Wireless Propagation Letters **15**, 484 (2016).
[4] G. Valerio, Z. Sipus, A. Grbic, and O. Quevedo-Teruel, IEEE Transactions on Antennas and Propagation **65**, 2695 (2017).
[5] O. Dahlberg, R. C. Mitchell-Thomas, and O. Quevedo-Teruel, Scientific Reports **7**, 10136 (2017).
[6] J. A. Dockrey, M. J. Lockyear, S. J. Berry, S. A. R. Horsley, J. R. Sambles, and A. P. Hibbins, Physical Review B **87**, 125137 (2013).
[7] F. Monticone and A. Alù, Proceedings of the IEEE **103**, 793 (2015).
[8] O. Quevedo-Teruel, Progress In Electromagnetics Research **140**, 169 (2013).
[9] M. Ebrahimpouri, E. Rajo-Iglesias, Z. Sipus, and O. Quevedo-Teruel, in *2016 10th European Conference on Antennas and Propagation, EuCAP 2016* (IEEE, 2016) pp. 1–2.
[10] M. Ebrahimpouri, O. Quevedo-Teruel, and E. Rajo-Iglesias, IEEE Microwave and Wireless Components Letters **27**, 542 (2017).
[11] M. Camacho, R. C. Mitchell-Thomas, A. P. Hibbins, J. Roy Sambles, and O. Quevedo-Teruel, Optics Letters **42**, 3375 (2017).
[12] M. Memarian and G. V. Eleftheriades, Nature communications **6**, 5855 (2015).
[13] D. R. Jackson, C. Caloz, and T. Itoh, Proceedings of the IEEE **100**, 2194 (2012).
[14] M. Xiao, G. Ma, Z. Yang, P. Sheng, Z. Q. Zhang, and C. T. Chan, Nature Physics **11**, 240 (2015), arXiv:1411.7100.
[15] M. Xiao, Z. Q. Zhang, and C. T. Chan, Physical Review X **4**, 021017 (2014), arXiv:1401.1309.
[16] C. Wen, IEEE Transactions on Microwave Theory and Techniques **17**, 1087 (1969).
[17] W. R. Deal, IEEE Microwave Magazine **9**, 120 (2008).
[18] O. Quevedo-Teruel and A. Neto, in *Proceedings of the 5th European Conference on Antennas and Propagation (EUCAP)* (2011) pp. 3527–3530.
[19] "CST Microwave Studio," http://www.cst.com.
[20] M. Camacho, R. R. Boix, F. Medina, A. P. Hibbins, and J. R. Sambles, Physical Review B **95**, 245425 (2017).
[21] A. Neto and S. Maci, IEEE Transactions on Antennas and Propagation **51**, 1572 (2003).